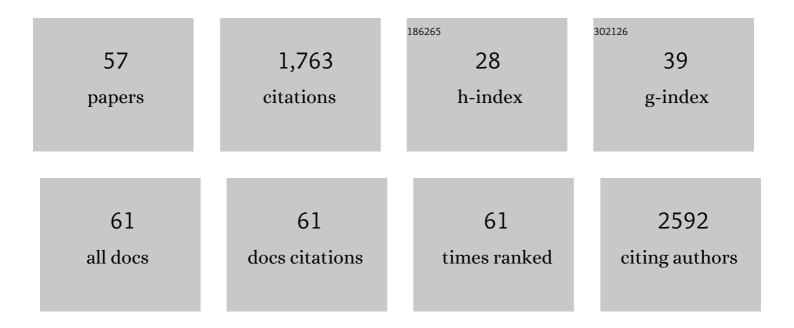
## Julien Valette

List of Publications by Year in descending order

Source: https://exaly.com/author-pdf/3385588/publications.pdf Version: 2024-02-01



LILLEN VALETTE

#	Article	lF	CITATIONS
1	Using spectrally-selective radiofrequency pulses to enhance lactate signal for diffusion-weighted MRS measurements in vivo. Journal of Magnetic Resonance, 2022, 334, 107113.	2.1	2
2	Magnetic resonance spectroscopy in the rodent brain: Experts' consensus recommendations. NMR in Biomedicine, 2021, 34, e4325.	2.8	9
3	Characterizing extracellular diffusion properties using diffusionâ€weighted MRS of sucrose injected in mouse brain. NMR in Biomedicine, 2021, 34, e4478.	2.8	5
4	Inflammationâ€driven glial alterations in the cuprizone mouse model probed with diffusionâ€weighted magnetic resonance spectroscopy at 11.7 T. NMR in Biomedicine, 2021, 34, e4480.	2.8	7
5	Revisiting double diffusion encoding MRS in the mouse brain at 11.7T: Which microstructural features are we sensitive to?. Neurolmage, 2020, 207, 116399.	4.2	13
6	Complementarity of gluCEST and <sup>1</sup> Hâ€MRS for the study of mouse models of Huntington's disease. NMR in Biomedicine, 2020, 33, e4301.	2.8	14
7	Longitudinal characterization of cognitive and motor deficits in an excitotoxic lesion model of striatal dysfunction in non-human primates. Neurobiology of Disease, 2019, 130, 104484.	4.4	8
8	Diffusion-weighted magnetic resonance spectroscopy enables cell-specific monitoring of astrocyte reactivity in vivo. Neurolmage, 2019, 191, 457-469.	4.2	42
9	The striatal kinase DCLK3 produces neuroprotection against mutant huntingtin. Brain, 2018, 141, 1434-1454.	7.6	23
10	Can we detect the effect of spines and leaflets on the diffusion of brain intracellular metabolites?. Neurolmage, 2018, 182, 283-293.	4.2	37
11	Insights into brain microstructure from in vivo DW-MRS. NeuroImage, 2018, 182, 97-116.	4.2	62
12	Efficient GPU-based Monte-Carlo simulation of diffusion in real astrocytes reconstructed from confocal microscopy. Journal of Magnetic Resonance, 2018, 296, 188-199.	2.1	15
13	Brain Metabolite Diffusion from Ultra-Short to Ultra-Long Time Scales: What Do We Learn, Where Should We Go?. Frontiers in Neuroscience, 2018, 12, 2.	2.8	20
14	In Vivo Multidimensional Brain Imaging in Huntington's Disease Animal Models. Methods in Molecular Biology, 2018, 1780, 285-301.	0.9	0
15	Imaging and spectroscopic approaches to probe brain energy metabolism dysregulation in neurodegenerative diseases. Journal of Cerebral Blood Flow and Metabolism, 2017, 37, 1927-1943.	4.3	24
16	Using 31P-MRI of hydroxyapatite for bone attenuation correction in PET-MRI: proof of concept in the rodent brain. EJNMMI Physics, 2017, 4, 16.	2.7	1
17	Modeling diffusion of intracellular metabolites in the mouse brain up to very high diffusionâ€weighting: Diffusion in long fibers (almost) accounts for nonâ€monoexponential attenuation. Magnetic Resonance in Medicine, 2017, 77, 343-350.	3.0	47
18	Metabolite diffusion up to very high <i>b</i> in the mouse brain in vivo: Revisiting the potential correlation between relaxation and diffusion properties. Magnetic Resonance in Medicine, 2017, 77, 1390-1398.	3.0	28

JULIEN VALETTE

#	Article	IF	CITATIONS
19	Experimental strategies for inÂvivo 13 C NMR spectroscopy. Analytical Biochemistry, 2017, 529, 216-228.	2.4	17
20	Probing metabolite diffusion at ultraâ€short time scales in the mouse brain using optimized oscillating gradients and "shortâ€â€echoâ€ŧime diffusionâ€weighted MRS. NMR in Biomedicine, 2017, 30, e3671.	2.8	20
21	Energy defects in Huntington's disease: Why "inÂvivo―evidence matters. Biochemical and Biophysical Research Communications, 2017, 483, 1084-1095.	2.1	57
22	Paclitaxel-loaded PEGylated nanocapsules of perfluorooctyl bromide as theranostic agents. European Journal of Pharmaceutics and Biopharmaceutics, 2016, 108, 136-144.	4.3	34
23	In vivo imaging of brain glutamate defects in a knock-in mouse model of Huntington's disease. NeuroImage, 2016, 139, 53-64.	4.2	68
24	New paradigm to assess brain cell morphology by diffusion-weighted MR spectroscopy in vivo. Proceedings of the National Academy of Sciences of the United States of America, 2016, 113, 6671-6676.	7.1	81
25	Evidence for a "metabolically inactive―inorganic phosphate pool in adenosine triphosphate synthase reaction using localized 31P saturation transfer magnetic resonance spectroscopy in the rat brain at 11.7 T. Journal of Cerebral Blood Flow and Metabolism, 2016, 36, 1513-1518.	4.3	15
26	Alzheimer's disease-like APP processing in wild-type mice identifies synaptic defects as initial steps of disease progression. Molecular Neurodegeneration, 2016, 11, 5.	10.8	37
27	Brain intracellular metabolites are freely diffusing along cell fibers in grey and white matter, as measured by diffusion-weighted MR spectroscopy in the human brain at 7 T. Brain Structure and Function, 2016, 221, 1245-1254.	2.3	44
28	Gradient rotating outer volume excitation (GROOVE): A novel method for singleâ€shot twoâ€dimensional outer volume suppression. Magnetic Resonance in Medicine, 2015, 73, 139-149.	3.0	2
29	The Neuroprotective Agent CNTF Decreases Neuronal Metabolites in the Rat Striatum: An <i>in Vivo</i> Multimodal Magnetic Resonance Imaging Study. Journal of Cerebral Blood Flow and Metabolism, 2015, 35, 917-921.	4.3	21
30	Metabolic Modeling of Dynamic 13C NMR Isotopomer Data in the Brain In Vivo: Fast Screening of Metabolic Models Using Automated Generation of Differential Equations. Neurochemical Research, 2015, 40, 2482-2492.	3.3	11
31	RGD decoration of PEGylated polyester nanocapsules of perfluorooctyl bromide for tumor imaging: Influence of pre or post-functionalization on capsule morphology. European Journal of Pharmaceutics and Biopharmaceutics, 2014, 87, 170-177.	4.3	39
32	Intracellular metabolites in the primate brain are primarily localized in long fibers rather than in cell bodies, as shown by diffusion-weighted magnetic resonance spectroscopy. NeuroImage, 2014, 90, 374-380.	4.2	30
33	In vivo CEST MR imaging of U87 mice brain tumor angiogenesis using targeted LipoCEST contrast agent at 7 T. Magnetic Resonance in Medicine, 2013, 69, 179-187.	3.0	40
34	19F molecular MR imaging for detection of brain tumor angiogenesis: in vivo validation using targeted PFOB nanoparticles. Angiogenesis, 2013, 16, 171-179.	7.2	43
35	13C NMR spectroscopy applications to brain energy metabolism. Frontiers in Neuroenergetics, 2013, 5, 9.	5.3	29
36	Anomalous Diffusion of Brain Metabolites Evidenced by Diffusion-Weighted Magnetic Resonance Spectroscopy <i>in Vivo</i> . Journal of Cerebral Blood Flow and Metabolism, 2012, 32, 2153-2160.	4.3	43

JULIEN VALETTE

#	Article	IF	CITATIONS
37	pH as a Biomarker of Neurodegeneration in Huntington's Disease: A Translational Rodent-Human MRS Study. Journal of Cerebral Blood Flow and Metabolism, 2012, 32, 771-779.	4.3	39
38	Metabolic Modeling of Dynamic Brain 13C NMR Multiplet Data: Concepts and Simulations with a Two-Compartment Neuronal-Glial Model. Neurochemical Research, 2012, 37, 2388-2401.	3.3	21
39	A new sequence for singleâ€shot diffusionâ€weighted NMR spectroscopy by the trace of the diffusion tensor. Magnetic Resonance in Medicine, 2012, 68, 1705-1712.	3.0	31
40	Long-circulating perfluorooctyl bromide nanocapsules for tumor imaging by 19FMRI. Biomaterials, 2012, 33, 5593-5602.	11.4	69
41	High sensitivity <sup>19</sup> F MRI of a perfluorooctyl bromide emulsion: application to a dynamic biodistribution study and oxygen tension mapping in the mouse liver and spleen. NMR in Biomedicine, 2012, 25, 654-660.	2.8	36
42	In Vivo 13C Magnetic Resonance Spectroscopy and Metabolic Modeling: Methodology. Advances in Neurobiology, 2012, , 181-220.	1.8	3
43	A new paradigm for high-sensitivity <sup>19</sup> F magnetic resonance imaging of perfluorooctylbromide. Magnetic Resonance in Medicine, 2010, 63, 1119-1124.	3.0	53
44	About the origins of NMR diffusion-weighting induced by frequency-swept pulses. Journal of Magnetic Resonance, 2010, 205, 255-259.	2.1	13
45	Multimodal neuroimaging provides a highly consistent picture of energy metabolism, validating <sup>31</sup> P MRS for measuring brain ATP synthesis. Proceedings of the National Academy of Sciences of the United States of America, 2009, 106, 3988-3993.	7.1	47
46	Simplified <sup>13</sup> C metabolic modeling for simplified measurements of cerebral TCA cycle rate in vivo. Magnetic Resonance in Medicine, 2009, 62, 1641-1645.	3.0	7
47	Neurochemical changes in the rat prefrontal cortex following acute phencyclidine treatment: an <i>in vivo</i> localized <sup>1</sup> H MRS study. NMR in Biomedicine, 2009, 22, 737-744.	2.8	83
48	Diffusionâ€weighted NMR spectroscopy allows probing of <sup>13</sup> C labeling of glutamate inside distinct metabolic compartments in the brain. Magnetic Resonance in Medicine, 2008, 60, 306-311.	3.0	17
49	On the reliability of13C metabolic modeling with two-compartment neuronal-glial models. Journal of Neuroscience Research, 2007, 85, 3294-3303.	2.9	46
50	Spectroscopic imaging with volume selection by unpaired adiabatic π pulses: Theory and application. Journal of Magnetic Resonance, 2007, 189, 1-12.	2.1	8
51	Isoflurane Strongly Affects the Diffusion of Intracellular Metabolites, as Shown by 1H Nuclear Magnetic Resonance Spectroscopy of the Monkey Brain. Journal of Cerebral Blood Flow and Metabolism, 2007, 27, 588-596.	4.3	45
52	Neuron?astrocyte interactions in the regulation of brain energy metabolism: a focus on NMR spectroscopy. Journal of Neurochemistry, 2006, 99, 393-401.	3.9	51
53	Proton-observed carbon-edited NMR spectroscopy in strongly coupled second-order spin systems. Magnetic Resonance in Medicine, 2006, 55, 250-257.	3.0	58
54	B0 homogeneity throughout the monkey brain is strongly improved in the sphinx position as compared to the supine position. Journal of Magnetic Resonance Imaging, 2006, 23, 408-412.	3.4	9

JULIEN VALETTE

#	Article	IF	CITATIONS
55	Glycolysis versus TCA Cycle in the Primate Brain as Measured by Combining 18F-FDG PET and 13C-NMR. Journal of Cerebral Blood Flow and Metabolism, 2005, 25, 1418-1423.	4.3	33
56	Optimized diffusion-weighted spectroscopy for measuring brain glutamate apparent diffusion coefficient on a whole-body MR system. NMR in Biomedicine, 2005, 18, 527-533.	2.8	23
57	NMR measurement of brain oxidative metabolism in monkeys using13C-labeled glucose without a13C radiofrequency channel. Magnetic Resonance in Medicine, 2004, 52, 33-40.	3.0	43